Research Article Open Access

Regina Kruse, Christine Silberhorn, and Tim Bartley*

Heralded orthogonalisation of coherent states and their conversion to discrete-variable superpositions

https://doi.org/10.1515/qmetro-2017-0005
Received November 9, 2017; accepted November 28, 2017

Abstract: The nonorthogonality of coherent states is a fundamental property which prevents them from being perfectly and deterministically discriminated. Here, we present an experimentally feasible protocol for the probabilistic orthogonalisation of a pair of coherent states, independent of their amplitude and phase. In contrast to unambiguous state discrimination, a successful operation of our protocol is heralded without measuring the states. As such, they remain suitable for further manipulation and the obtained orthogonal states serve as a discrete-variable basis. Therefore, our protocol doubles as a simple continuous-to-discrete variable converter, which may find application in hybrid continuous-discrete quantum information processing protocols.

Keywords: photon statistics, state discrimination, measurement-induced nonclassicality

1 Introduction

One of the fundamental properties of coherent states is that they are over complete, i.e. each coherent state shares some non-zero overlap with every other. In the context of state discrimination, this non-zero overlap manifests as errors when one wishes to distinguish two such states. One option to try and discriminate between the two states is by a direct measurement (DM). However, as the two states share a finite overlap, we cannot obtain a result with absolute certainty. The limits of the DM approach are determined by a minimal error, the so-called Helstrom bound [1–6]. These errors can be overcome using established unambiguous state discrimination protocols [7]. The original proposals considered schemes in which nonorthogonal states were first orthogonalised, and then measured with a suitable detection scheme [8, 9]. However, for a valid implementation, these steps must be combined [10–21], such that orthogonalisation is post-selected on the appropriate measurement outcome, non-destructive [22, 23] or otherwise. Yet, in some cases it may be necessary to orthogonalise the input states without a post-selected measurement.

One application where this is needed is the conversion of continuous-variable (CV) to discrete-variable (DC) quantum states. In quantum information, hybrid approaches that utilise methods from both the CV and DV world offer significant advantages compared to pure CV or DV protocols [24, 25]. From a fundamental perspective, similar hybrid schemes have also been used to investigate phenomena such as micro-macro entanglement, in which a path-entangled photon (DV entanglement) is coherently displaced (a CV operation) [26–28]. By combining the best of both worlds, hybrid schemes can save on resources in teleportation, quantum computing and error correction schemes [29–32] or may reduce the effect of loss on the distribution of CV entanglement [33]. To obtain a functioning scheme, hybrid protocols require a reliable and efficient transfer of information from the continuous to the discrete part of the protocol [25, 34]. Recently, such a protocol has been proposed and demonstrated [35]. However, it relies critically on an entangled resource-state [31] and utilises a teleportation scheme [30], which leaves the question whether a more resource-efficient approach may be found.

In this paper, we develop a practical scheme for heralded, non-destructive state orthogonalisation of continuous-variable states, which doubles as a continuous-to-discrete-variable qubit converter. Our protocol describes the probabilistic transformation of non-orthogonal CV states, namely weak coherent states of opposite phase, to displaced DV states, i.e. $\hat{D}(\beta)(c_0|0\rangle + c_1|1\rangle)$, where β, c_0, c_1 depend on the inter-

Regina Kruse, Christine Silberhorn: Applied Physics, University of Paderborn, Warburger Straße 100, 33098 Paderborn, Germany
***Corresponding Author: Tim Bartley:** Applied Physics, University of Paderborn, Warburger Straße 100, 33098 Paderborn, Germany, E-mail: tim.bartley@upb.de

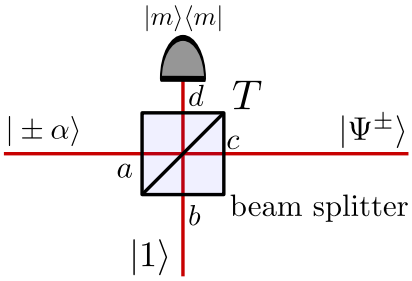

Figure 1: Photon replacement scheme for state discrimination. A coherent state from the set $\{|\alpha\rangle, |-\alpha\rangle\}$ is incident on one input mode of a beam splitter of predetermined transmissivity T. Incident on the other input mode is an ancilla photon. For suitably chosen transmissivity T, dependent on $|\alpha|$, a projective measurement of a particular photon number $|m\rangle\langle m|$ on one output mode transforms the initial set onto the orthogonal set of $\{|\Psi^+\rangle, |\Psi^-\rangle\}$ on the other output mode.

action parameters. These interaction parameters can be specified *a priori* to ensure that the resulting output states are orthogonal to one another. That is, the input states $\{|\psi\rangle, |-\psi\rangle\}$, where $\langle\psi|-\psi\rangle \neq 0$ transform to new states $\{|\psi'\rangle, |-\psi'\rangle\}$, whereby $\langle\psi'|-\psi'\rangle = 0$. Note that this is related but different to input state orthogonalisers [36–38], in which the output state is orthogonal to the input state, i.e. $|\psi\rangle \to |\psi'\rangle$ where $\langle\psi|\psi'\rangle = 0$.

Contrary to other orthogonalisation schemes, the conversion is heralded by a predetermined detection event without destroying the input state. To obtain the desired orthogonalisation, we utilise quantum-optical catalysis [39–42], where an ancilla photon interferes with a CV input state on a beam splitter and a predetermined detection event in one beam splitter output heralds the desired displaced DV state in the other output. As this procedure is coherent, it may also be used on single-mode coherent state superposition (CSS) states $|\Phi_{\text{Sup}}\rangle = \left(|\alpha\rangle + e^{i\phi}|-\alpha\rangle\right)$ that are considered the continuous variable equivalent of a qubit [43–46]. After transformation with our scheme, the new basis states of the superposition are orthogonal and may be mapped onto the basis states of a discrete variable system. Thus, our orthogonalisation protocol also comprises a continuous- to discrete-variable qubit converter.

This paper consists of three sections. We first present the scheme and its application in a state discrimination scenario and find the optimal parameters to discriminate between the two coherent states. In the second section, we look in more detail at the resulting states following this operation. It turns out that these states become extremely good approximations of discrete-variable superposition states. In the third section, we exploit the fact that our states are not destroyed after applying this operation to investigate the iterative operation, which can further increase the success probability.

2 Quantum catalysis for heralded state orthogonalisation

To implement our scheme, we utilise the "quantum catalysis" (or "photon replacement") technique [39–41], as depicted in Fig. 1. An input state from the non-orthogonal set $\{|\alpha\rangle, |-\alpha\rangle\}$ is incident on mode a of a beam splitter, simultaneously with an ancilla photon in mode b. Dependent on the amplitude of the coherent states $|\alpha|$, we pick the transmissivity of the beam splitter $T(|\alpha|)$ such that, given a particular outcome of a photon number measurement $|m\rangle\langle m|$ on one output mode of the beam splitter, the input state is projected on either $|\Psi^+\rangle$ or $|\Psi^-\rangle$, depending on the sign of the incident coherent state. The transformation coefficients of an n-photon Fock state for this replacement operation are then given via

$$|\Psi_{\text{out}}\rangle = \sqrt{\frac{m!(n+k-m)!}{n!k!}} \sum_{j=0}^{k} \binom{n}{m-j} \binom{k}{j} (-1)^j \times \sqrt{T}^{n-m+2j} \sqrt{1-T}^{m+k-2j} |n+k-m\rangle_c \otimes |m\rangle_d \,, \tag{1}$$

with, in general, k ancilla and m herald photons for the success event. The transformation of the incident coherent states can then be calculated with the photon number basis representation $|\alpha\rangle = \sum_{n=0}^{\infty} e^{-\frac{\alpha}{2}} \frac{\alpha^n}{\sqrt{n!}} |n\rangle$.

As an example, let us consider the case sketched in Fig. 1. At the replacement stage, we define a success event such that one photon is heralded in mode d, i.e. $|m\rangle\langle m| = |1\rangle\langle 1|$. The final output state $|\Psi^{\pm}\rangle$ is given by

$$|\Psi^{\pm}\rangle = \frac{1}{\sqrt{\mathcal{N}}} \exp\left(-\frac{|\alpha|^2}{2}\right) \exp\left(\pm\alpha\sqrt{T}\hat{c}^{\dagger}\right) \times \left(\pm\alpha(1-T)\hat{c}^{\dagger} - \sqrt{T}\right) |0\rangle_c \otimes |1\rangle_d \tag{2}$$

where $\sqrt{\mathcal{N}}$ is the normalisation after the non-unitary transformation and the probability of this event happening is given by $\mathcal{N} = \sum_{n=0}^{\infty} c_n^2(\text{repl.})$ with $c_n(\text{repl.}) = e^{-\frac{\alpha}{2}} \frac{\alpha^n}{\sqrt{n!}} \sqrt{T}^{n-1} [T - n(1-T)]$ as the state coefficients in the photon number basis. A more detailed discussion about the output states can be found in e.g. [39–41]. Writing the output state of the replacement stage in this form illustrates how the state orthogonalisation is possible with this protocol. Calculating the overlap $|\langle\Psi^+|\Psi^-\rangle|$ and setting it to zero yields a quadratic equation with (at least) one real valued solution due to the different signs of α (a closed-form expression for $T(|\alpha|)$ is given in the Appendix).

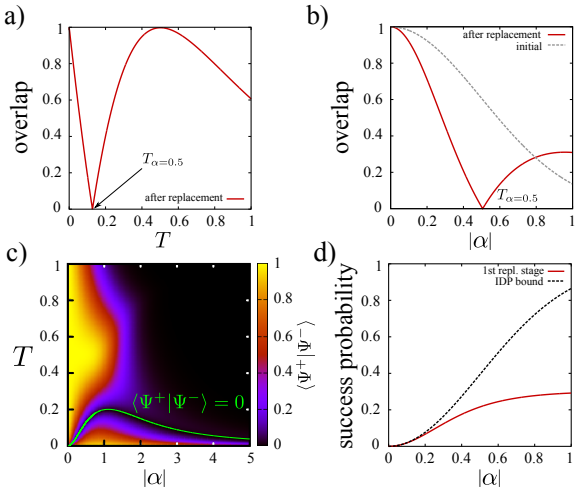

Figure 2: Overlap after the first replacement stage. Figure (a) shows the overlap after the replacement stage (red) for a fixed amplitude $|\alpha| = 0.5$ depending on the beam splitter transmissivity T. In figure (b) the overlap after replacement (red) is plotted dependent on $|\alpha|$ for a fixed transmissivity. For comparison the initial overlap is given in gray. In figure (c), we consider both the coherent state amplitude $|\alpha|$ and beam splitter transmissivity T as parameters for the replacement. In green we sketch the line of zero overlap, indicating the optimal beam splitter transmissivity $T(|\alpha|)$ for each $|\alpha|$. Figure (d) depicts the success probability for the first stage of a state discrimination protocol in red compared to the IDP bound in black. For details, see text.

This behaviour is shown in Fig. 2 (a). In red, we plot the overlap

$$|\langle\Psi^+|\Psi^-\rangle| = e^{-(T+1)|\alpha|^2} \times \left[(1-T)^2 T|\alpha|^4 - (1-3T)(1-T)|\alpha|^2 + T\right]$$

after the replacement stage versus the beam splitter transmissivity T. From a transmissivity of $T = 0$, we start with an overlap of one, as the beam splitter acts as a mirror and the ancilla photon exits the replacement stage in each case. Increasing the transmissivity, we find that the overlap decreases drastically, before it reaches zero at $T(|\alpha| = 0.5) = 0.13$. This situation fulfils the aim of the protocol; it is the required beam splitter transmissivity to distinguish states $|+\alpha\rangle$, $|-\alpha\rangle$ for $|\alpha| = 0.5$. Although the shape of the overlap curve is quite steep at this point, this does not pose an insurmountable experimental challenge since the transmissivity of a beam splitter may be finely controlled. Going further to $T = 1$, the overlap increases to the initial overlap of $|\langle-\alpha|\alpha\rangle| = 0.6$ as the initial states are directly transmitted. In Fig. 2 (b), we consider the overlap after replacement for $T(|\alpha| = 0.5) = 0.13$ in red. Compared to the initial overlap $|\langle-\alpha|\alpha\rangle|$ sketched in gray, the overlap of the replaced state drops off faster for small amplitudes $|\alpha|$, before it reaches zero at $|\alpha| = 0.5$.

In Fig. 2(c), we consider the full parameter space for the replacement. We calculate and plot the overlap after replacement depending on the coherent state amplitude $|\alpha|$ and the beam splitter transmissivity T. For high amplitudes and splitter transmissivities, we find a large region where the overlap is very small. However, only for the combination of coherent state amplitudes and transmissivities that are represented by the green line the overlap becomes zero. Since this is the goal of the state discrimination, this curve defines the appropriate beam splitter transmissivity $T(|\alpha|)$ for any given $|\alpha|$ in the protocol. The sensitivity of the scheme to the control of the transmissivity can be seen in the gradient of the colour map in Fig. 2(c): it is much sharper at low $|\alpha|$, indicating higher sensitivity to errors in controlling T. The corresponding probability of success, i.e. the probability of detecting a desired heralding event is plotted in Fig. 2(d). For each amplitude $|\alpha|$, we calculated the optimal transmissivity $T(|\alpha|)$, where $|\langle\Psi^+|\Psi^-\rangle| = 0$. Further details are provided in the Appendix. From the photon number coefficients c_n(repl.), we have then determined the success probability shown in red. Comparing the success probability to the IDP bound (black) from unambiguous state discrimination for small $|\alpha|$, we find that we already operate close to the optimum predicted for probabilistic discrimination protocols. However, for larger amplitudes we are still some way from optimal operation.

3 Projection on displaced discrete variable qubit states

It is instructive to ask the nature of the state once it has undergone a successful discrimination operation. In Fig. 3 we plot the Wigner function of the state $|\psi^+\rangle$ when $\alpha = 0.5$ and $T = 0.13$, the parameters required to discriminate the state from $|\psi^-\rangle$. This state has a fidelity of >98% with the state $\frac{1}{\sqrt{2}}(|0\rangle - |1\rangle)$. Similarly, the state $|\psi^-\rangle$, for which $\alpha = -1/2$ for the same T, shares >98% fidelity with the state $\frac{1}{\sqrt{2}}(|0\rangle + |1\rangle)$. Thus the discrimination operation heralds the generation of a close approximation to the state $|\alpha\rangle \Rightarrow \frac{1}{\sqrt{2}}(|0\rangle - |1\rangle)$ and $|-\alpha\rangle \Rightarrow \frac{1}{\sqrt{2}}(|0\rangle + |1\rangle)$ with reasonable fidelity.

With these transformations in mind, we consider the transformations of superpositions of coherent states as inputs. The even coherent state superposition (CSS) state $|\alpha\rangle + |-\alpha\rangle$, with amplitude $|\alpha| = 0.5$, transforms into the state $|\psi^+\rangle + |\psi^-\rangle$, the Wigner function of which is shown Fig. 4 (a). Under the conditions for orthogonalised output states, i.e. $T = 0.13$, this state has a fidelity of 96% with

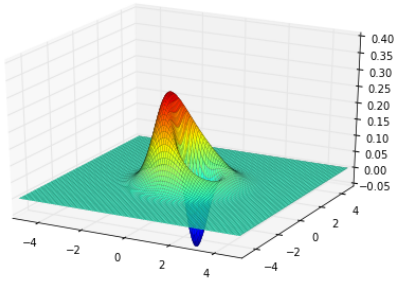

Figure 3: Wigner function of transformed state $|\psi^+\rangle$. This state has a fidelity >98% with the discrete-variable equal superposition state $\frac{1}{\sqrt{2}}(|0\rangle - |1\rangle)$

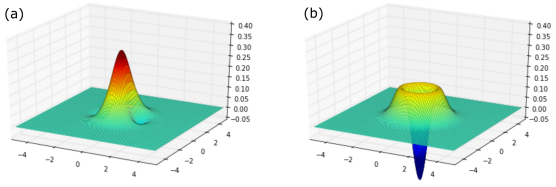

Figure 4: Wigner functions of (a) transformed state $|\alpha\rangle + |-\alpha\rangle \Rightarrow |\psi^+\rangle - |\psi^-\rangle$ and (b) transformed state $|\alpha\rangle - |-\alpha\rangle \Rightarrow |\psi^+\rangle + |\psi^-\rangle$. These states have > 99% fidelity to the weakly squeezed vacuum and single-photon Fock states, respectively.

the vacuum state $|0\rangle$, but >99% fidelity with the squeezed vacuum state (squeezed by 2.4 dB). Similarly, the odd CSS state $|\alpha\rangle - |-\alpha\rangle$ transforms to the state $|\psi^+\rangle - |\psi^-\rangle$, shown in Fig. 4, which exhibits >99.9% fidelity to the single photon Fock state.

More generally, we can rewrite the state generated by the successful interaction from Eq. 2 as a displaced discrete-variable superposition state, i.e.

$$|\Psi^{\pm}\rangle = \hat{D}\left(\pm\alpha\sqrt{T}\right)\left[c_0(\alpha)|0\rangle + c_1(\alpha)|1\rangle\right] \tag{3}$$

with the (unnormalised) coefficients given by $c_0(\alpha) = \sqrt{T}\left[1-(1-T)|\alpha|^2\right]$ and $c_1(\alpha) = -(1-T)\alpha$. From this, one can calculate a value of $T(|\alpha|)$ for which the displaced equal superposition state $D(\beta)\left(|0\rangle + e^{i\phi}|1\rangle\right)$ is generated; a full expression is given the appendix for completeness. Note that this value of T is not the same as that which discriminates the states, since, in general, displaced superpositions are nonorthogonal.

Similarly, the output state after acting on a even and odd CSS states is the coherent superposition of the individual output states in Eq. 3, i.e.

$$\begin{aligned}|\alpha\rangle \pm |-\alpha\rangle \rightarrow & \hat{D}\left(\alpha\sqrt{T}\right)\left[c_0|0\rangle + c_1(\alpha)|1\rangle\right] \\ & \pm \hat{D}\left(-\alpha\sqrt{T}\right)\left[c_0|0\rangle + c_1(-\alpha)|1\rangle\right] \\ = & c_0\left[\hat{D}\left(\alpha\sqrt{T}\right) \pm \hat{D}\left(-\alpha\sqrt{T}\right)\right]|0\rangle \\ & + c_1(\alpha)\left[\hat{D}\left(\alpha\sqrt{T}\right) \mp \hat{D}\left(-\alpha\sqrt{T}\right)\right]|1\rangle\end{aligned} \tag{4}$$

where the coefficients c_0 and $c_1(\alpha)$ are as before, and we use $c_1(-\alpha) = -c_1(\alpha)$. This state is a hybrid CV-DV state; the coherent superposition of positive and negative displacements (a non-Gaussian CV operation) act on the superposition of the single-rail DV qubit state $c_0|0\rangle + c_1|1\rangle$, with $c_{0,1}$ determined by the interaction parameters. Indeed, this can be seen as the single-rail analogue of the entangled state produced by Ulanov *et al.* in Ref. [35]. Of course, this state requires CSS states as an input, the generation of which remains challenging, notwithstanding substantial experimental progress in both the optical [47–50] and superconducting circuit [51] domains.

4 Iterative operation

In contrast to conventional protocols, we have the advantage that our protocol does not destroy the input state, even in case of failure. We can therefore further operate on the state to try to obtain the desired states. With the information we gain from the heralding event, we can feed forward to subsequent stages to try and recover the desired states. However, due to the large number of possible detection events ($|0\rangle\langle 0|, |1\rangle\langle 1|, |2\rangle\langle 2|$...) the output states that condition the adaptation of the protocol span a large space. Here, we consider optimising iterative operation of the protocol to target orthogonal states; we restrict ourselves to a few specific examples of failure modes and will not exhaust the full parameter space of cascading multiple stages with multiple failure modes.

In particular as sketched in Fig. 5(a), we only consider two detection events as valid and discard the rest. Let us start with a known $|\alpha|$ at the first replacement stage. Here, we consider heralding on one photon as success and measuring vacuum as failure. Other events, such as detecting 2, 3 or more photons are consequently discarded and the protocol aborted. The failure state from heralding on vacuum is known and we can already prepare the second stage to reattempt to obtain orthogonal states. That is, we can determine the success and failure event of the second stage and adjust the splitter transmissivity accordingly. Going one step further, we then also know the state

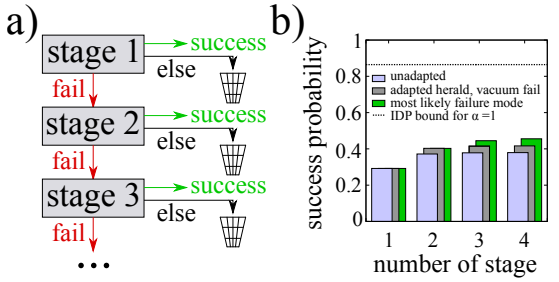

Figure 5: Cascading of replacement stages. Figure (a) shows the cascading strategy. We consider only one success and one failure heralding event. In any other case, we abort the protocol. In figure (b), we depict the probability of success for three different cascading protocols with $|\alpha| = 1.0$. The unadapted protocol (lilac) considers just repeating the first stage with modified transmissivity. The only considered failure mode is vacuum. In grey, we show the success probabilities for a protocol with adapted success events. In this case, only the vacuum is considered as failure mode. The probabilities presented in green are calculated from a protocol that both adapts the success and failure mode to the most likely event at each stage. In all cases, detection outcomes apart from the success and selected failure mode are discarded.

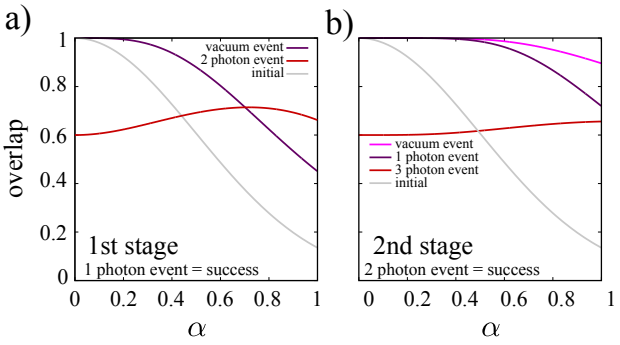

Figure 6: Overlap of the photon-replaced states when detecting a failure event. In both figures we have plotted the initial overlap between the two stages in grey. Figure (a) shows the overlap after the first stage for the two most likely failure events, i.e. detecting vacuum in purple and heralding on two photons in red. After a vacuum event in the first stage, we also consider the overlap for different failure modes in the second stage in figure (b). For details, see text.

after the second failure event and can adjust the third stage etc.

In Fig. 5 (b), we consider three of these cascading protocols to optimise the success probability for a given amplitude $|\alpha| = 1.0$. A simple example is the repetition of the first replacement stage, i.e. using one photon as an ancilla and heralding on one photon for success. As the single failure event, we consider measuring vacuum in mode d. However, this simple protocol does not give the highest success probability. We can improve it by adapting the success event to the stage number such that we herald on increasing photon number. This means, in stage one we herald on $|1\rangle\langle 1|$, in stage two on $|2\rangle\langle 2|$ and so on. This approach conserves the photon number between initial and output state if we consider measuring vacuum as the single failure mode [1]. While this protocol gives higher success probability as sketched in gray, it is still possible to improve. In green, we have sketched the success probabilities when also adapting the failure mode from vacuum to measuring one photon less than required for the success event. This is the most likely failure event at any given stage of the protocol. As the success probabilities for the higher stage numbers scale with the failure probabilities in the previous ones, choosing a more likely failure event will increase the overall success efficiency.

However, in each of the depicted protocols in Fig. 5 we do not reach the IDP bound in black. Extrapolating the success probabilities, we assume that the considered cases do not reach the optimal success probability of state discrimination, even in the limit of many stages. However, we have not considered the possibility of other failure modes due to the large parameter space. When considering those, we are likely to improve the overall success probability, however it remains to be seen whether a generalisation of this particular protocol indeed reaches the appropriate bound [8].

We also note some interesting behaviour of the overlap between the output states behaves in the cases where we detect a failure event. In general, when a state discrimination protocol fails, the overlap after the failure event will be higher than before [7, 52]. In the case of optimal success probability (IDP), a failure will project the two initial states onto the same output state and consequently prohibit any further attempts to distinguish [8, 9]. In our case, we have more than one failure mode for which we may consider the overlap after replacement. In Fig. 6, we plot the overlap for different failure events in the first and second stage compared to the initial overlap. Let us consider the overlap after the first stage in Fig. 6(a). For comparison, the initial overlap (grey) between the states $\langle -\alpha|\,\alpha\rangle$ is depicted dependent on $|\alpha|$. In case of measuring vacuum (shown in purple), the overlap after the replacement increases as expected. Especially in the case of low coherent state amplitudes $|\alpha| \lesssim 0.2$, where the success probability is close to the IDP limit, the overlap after the transfor-

1 Strictly speaking, the mean photon number of the input state is changed by the non-unitary operation. However, this approach conserves photon number with respect to the total number of input ancilla photons and output (heralding) measured photons.

mation approaches unity. This behaviour prohibits further distinguishing of the states, as expected.

The interesting case occurs when we detect more photons than necessary for the success event, i.e. more than one in the first stage. Then, for small coherent state amplitudes the overlap *decreases* compared to the initial states. This is atypical for state discrimination protocols and we attribute this effect to the presence of many failure modes where the overlap after failure can be "distributed" among them. To verify that this is not only true for this special case in the first stage, we also compare the overlap after the second replacement stage in Fig. 6(b). In this case, both the vacuum case (pink) and single photon herald case (purple) show an increase in overlap compared to the initial state (grey). However, when detecting a higher photon number than required for the success event (here: three photons (red)) the protocol behaves atypically and the overlap decreases.

5 Conclusion

In conclusion, we have proposed and discussed a scheme for practical heralded state discrimination. We have shown that for each coherent state amplitude $|\alpha|$ we can find a beam splitter transmissivity $T(|\alpha|)$ such that $\{|\alpha\rangle, |-\alpha\rangle\}$ is probabilistically mapped onto an orthogonal set $\{|\Psi^+\rangle, |\Psi^-\rangle\}$. We have discussed the success probability of such a scheme for cascaded replacement stages and have observed that the overlap after replacement behaves differently to USD for certain failure modes. The success probability is closest to optimal at low $|\alpha|$, when the coherent states share large overlap initially. At larger coherent state amplitudes, interaction parameters can still be found to orthogonalise the states, however there is already minimal initial overlap in this regime, and the amount of failure modes increases since there are more photons involved in the interaction, resulting in a reduced probability from the optimal case. From these transformations, we have shown that one can construct a heralded coherent converter from continuous-variable coherent states to discrete-variable superposition states, and from coherent state superpositions to eigenstates of the photon number basis with reasonably high fidelities. This makes this operation an interesting and potentially useful tool in hybrid quantum information processing.

Acknowledgement: The authors thank D. Sych and M. Vanner for discussions. R.K. received financial support from the European Union's Horizon 2020 research and innovation program under the QCUMbER project Grant number 665148. T.J.B. acknowledges financial support from the DFG (Deutsche Forschungsgemeinschaft) under SFB/TRR 142.

References

[1] Carl W. Helstrom. *Quantum Detection and Estimation Theory*. Academic Press, January 1976.

[2] R. S. Kennedy. A near-optimum receiver for the binary coherent state quantum channel. *MIT Res. Lab. Electron. Quart. Progr. Rep.*, 110:219–225, 1972.

[3] S.J. Dolinar. An optimum receiver for the binary coherent state quantum channel. *MIT Res. Lab. Electron. Quart. Progr. Rep.*, 111:115–120, 1973.

[4] Christoffer Wittmann, Masahiro Takeoka, Katiúscia N. Cassemiro, Masahide Sasaki, Gerd Leuchs, and Ulrik L. Andersen. Demonstration of Near-Optimal Discrimination of Optical Coherent States. *Physical Review Letters*, 101(21):210501, November 2008.

[5] Denis Sych and Gerd Leuchs. Practical receiver for optimal discrimination of binary coherent signals. *Phys. Rev. Lett.*, 117:200501, Nov 2016.

[6] Christian R. Müller and Christoph Marquardt. A robust quantum receiver for phase shift keyed signals. *New Journal of Physics*, 17(3):032003, March 2015. arXiv: 1412.6242.

[7] I. D. Ivanovic. How to differentiate between non-orthogonal states. *Physics Letters A*, 123(6):257–259, August 1987.

[8] D. Dieks. Overlap and distinguishability of quantum states. *Physics Letters A*, 126(5–6):303–306, January 1988.

[9] Asher Peres. How to differentiate between non-orthogonal states. *Physics Letters A*, 128(1–2):19, March 1988.

[10] Miloslav Dušek, Mika Jahma, and Norbert Lütkenhaus. Unambiguous state discrimination in quantum cryptography with weak coherent states. *Physical Review A*, 62(2):022306, July 2000.

[11] Roger B. M. Clarke, Anthony Chefles, Stephen M. Barnett, and Erling Riis. Experimental demonstration of optimal unambiguous state discrimination. *Physical Review A*, 63(4):040305, March 2001.

[12] Luis Roa, Juan Carlos Retamal, and Carlos Saavedra. Quantum-state discrimination. *Physical Review A*, 66(1):012103, July 2002.

[13] Stephen M. Barnett, Anthony Chefles, and Igor Jex. Comparison of two unknown pure quantum states. *Physics Letters A*, 307(4):189–195, February 2003.

[14] Peter van Loock, Kae Nemoto, William J. Munro, Philippe Raynal, and Norbert Lütkenhaus. Implementing nonprojective measurements via linear optics: An approach based on optimal quantum-state discrimination. *Physical Review A*, 73(6):062320, June 2006.

[15] Michal Sedlák, Mário Ziman, Ondřej Přibyla, Vladimír Bužek, and Mark Hillery. Unambiguous identification of coherent states: Searching a quantum database. *Physical Review A*, 76(2):022326, August 2007.

[16] O. Jiménez, X. Sánchez-Lozano, E. Burgos-Inostroza, A. Delgado, and C. Saavedra. Experimental scheme for unambiguous dis-

crimination of linearly independent symmetric states. *Physical Review A*, 76(6):062107, December 2007.

[17] Luis Roa, M. L. Ladrón de Guevara, and A. Delgado. Conclusive modification of the overlap between two quantum states. *Physical Review A*, 81(3):034101, March 2010.

[18] Luis Roa, J. C. Retamal, and M. Alid-Vaccarezza. Dissonance is Required for Assisted Optimal State Discrimination. *Physical Review Letters*, 107(8):080401, August 2011.

[19] Kenji Nakahira and Tsuyoshi Sasaki Usuda. Optimal receiver for discrimination of two coherent states with inconclusive results. *Physical Review A*, 86(5):052323, November 2012.

[20] Bo Li, Shao-Ming Fei, Zhi-Xi Wang, and Heng Fan. Assisted state discrimination without entanglement. *Physical Review A*, 85(2):022328, February 2012.

[21] Luis Roa, Alejandra Maldonado-Trapp, Cristian Jara-Figueroa, and María Loreto L de Guevara. Quantum Discord Underlies the Optimal Scheme for Modifying the Overlap between Two States. *Journal of the Physical Society of Japan*, 83(4):044006, March 2014.

[22] Janos Bergou, Edgar Feldman, and Mark Hillery. Extracting information from a qubit by multiple observers: Toward a theory of sequential state discrimination. *Phys. Rev. Lett.*, 111:100501, Sep 2013.

[23] M. A. Solís-Prosser, P. González, J. Fuenzalida, S. Gómez, G. B. Xavier, A. Delgado, and G. Lima. Experimental multiparty sequential state discrimination. *Phys. Rev. A*, 94:042309, Oct 2016.

[24] Gershon Kurizki, Patrice Bertet, Yuimaru Kubo, Klaus Mølmer, David Petrosyan, Peter Rabl, and Jörg Schmiedmayer. Quantum technologies with hybrid systems. *PNAS*, 112(13):3866–3873, March 2015.

[25] Ulrik L. Andersen, Jonas S. Neergaard-Nielsen, Peter van Loock, and Akira Furusawa. Hybrid discrete- and continuous-variable quantum information. *Nat Phys*, 11(9):713–719, September 2015.

[26] N. Bruno, A. Martin, P. Sekatski, N. Sangouard, R. T. Thew, and N. Gisin. Displacement of entanglement back and forth between the micro and macro domains. *Nat Phys*, 9(9):545–548, September 2013.

[27] A. I. Lvovsky, R. Ghobadi, A. Chandra, A. S. Prasad, and C. Simon. Observation of micro-macro entanglement of light. *Nat Phys*, 9(9):541–544, September 2013.

[28] Ulrik L. Andersen and Jonas S. Neergaard-Nielsen. Heralded generation of a micro-macro entangled state. *Phys. Rev. A*, 88:022337, Aug 2013.

[29] Kimin Park, Seung-Woo Lee, and Hyunseok Jeong. Quantum teleportation between particlelike and fieldlike qubits using hybrid entanglement under decoherence effects. *Phys. Rev. A*, 86:062301, Dec 2012.

[30] Shuntaro Takeda, Takahiro Mizuta, Maria Fuwa, Peter van Loock, and Akira Furusawa. Deterministic quantum teleportation of photonic quantum bits by a hybrid technique. *Nature*, 500(7462):315–318, August 2013.

[31] Seung-Woo Lee and Hyunseok Jeong. Near-deterministic quantum teleportation and resource-efficient quantum computation using linear optics and hybrid qubits. *Phys. Rev. A*, 87(2):022326, February 2013.

[32] Guo Qi, Cheng Liu-Yong, Wang Hong-Fu, and Zhang Shou. Universal quantum computation using all-optical hybrid encoding. *Chinese Phys. B*, 24(4):040303, 2015.

[33] Alexander E. Ulanov, Ilya A. Fedorov, Anastasia A. Pushkina, Yury V. Kurochkin, Timothy C. Ralph, and A. I. Lvovsky. Undoing the effect of loss on quantum entanglement. *Nat Photon*, 9(11):764–768, November 2015.

[34] S. Pirandola, J. Eisert, C. Weedbrook, A. Furusawa, and S. L. Braunstein. Advances in quantum teleportation. *Nat Photon*, 9(10):641–652, October 2015.

[35] Alexander E. Ulanov, Demid Sychev, Anastasia A. Pushkina, Ilya A. Fedorov, and A. I. Lvovsky. Quantum Teleportation Between Discrete and Continuous Encodings of an Optical Qubit. *Phys. Rev. Lett.*, 118(16):160501, April 2017.

[36] M. R. Vanner, M. Aspelmeyer, and M. S. Kim. Quantum state orthogonalization and a toolset for quantum optomechanical phonon control. *Phys. Rev. Lett.*, 110:010504, Jan 2013.

[37] M. Ježek, M. Mičuda, I. Straka, M. Miková, M. Dušek, and J. Fiurášek. Orthogonalization of partly unknown quantum states. *Phys. Rev. A*, 89(4):042316, April 2014.

[38] Antonio S. Coelho, Luca S. Costanzo, Alessandro Zavatta, Catherine Hughes, M. S. Kim, and Marco Bellini. Universal Continuous-Variable State Orthogonalizer and Qubit Generator. *Phys. Rev. Lett.*, 116(11):110501, March 2016.

[39] A. I. Lvovsky and J. Mlynek. Quantum-Optical Catalysis: Generating Nonclassical States of Light by Means of Linear Optics. *Physical Review Letters*, 88(25):250401, June 2002.

[40] Kaoru Sanaka, Kevin J. Resch, and Anton Zeilinger. Filtering out photonic fock states. *Physical Review Letters*, 96(8):083601, February 2006.

[41] Tim J. Bartley, Gaia Donati, Justin B. Spring, Xian-Min Jin, Marco Barbieri, Animesh Datta, Brian J. Smith, and Ian A. Walmsley. Multiphoton state engineering by heralded interference between single photons and coherent states. *Physical Review A*, 86(4):043820, October 2012.

[42] Liyun Hu, Zeyang Liao, and M. Suhail Zubairy. Continuous-variable entanglement via multiphoton catalysis. *Phys. Rev. A*, 95(1):012310, January 2017.

[43] P. T. Cochrane, G. J. Milburn, and W. J. Munro. Macroscopically distinct quantum-superposition states as a bosonic code for amplitude damping. *Phys. Rev. A*, 59:2631–2634, Apr 1999.

[44] H. Jeong and M. S. Kim. Efficient quantum computation using coherent states. *Phys. Rev. A*, 65:042305, Mar 2002.

[45] T. C. Ralph, A. Gilchrist, G. J. Milburn, W. J. Munro, and S. Glancy. Quantum computation with optical coherent states. *Phys. Rev. A*, 68:042319, Oct 2003.

[46] A. P. Lund, T. C. Ralph, and H. L. Haselgrove. Fault-tolerant linear optical quantum computing with small-amplitude coherent states. *Phys. Rev. Lett.*, 100:030503, Jan 2008.

[47] Hiroki Takahashi, Kentaro Wakui, Shigenari Suzuki, Masahiro Takeoka, Kazuhiro Hayasaka, Akira Furusawa, and Masahide Sasaki. Generation of Large-Amplitude Coherent-State Superposition via Ancilla-Assisted Photon Subtraction. *Phys. Rev. Lett.*, 101(23):233605, December 2008.

[48] Thomas Gerrits, Scott Glancy, Tracy S. Clement, Brice Calkins, Adriana E. Lita, Aaron J. Miller, Alan L. Migdall, Sae Woo Nam, Richard P. Mirin, and Emanuel Knill. Generation of optical coherent-state superpositions by number-resolved photon subtraction from the squeezed vacuum. *Phys. Rev. A*, 82(3):031802, September 2010.

[49] Ruifang Dong, Anders Tipsmark, Amine Laghaout, Leonid A. Krivitsky, Miroslav Ježek, and Ulrik Lund Andersen. Generation of picosecond pulsed coherent state superpositions. *J. Opt. Soc.*

Am. B, JOSAB, 31(5):1192–1201, May 2014.

[50] Demid V. Sychev, Alexander E. Ulanov, Anastasia A. Pushkina, Matthew W. Richards, Ilya A. Fedorov, and A. I. Lvovsky. Breeding the optical Schroedinger's cat state. *arXiv:1609.08425 [quant-ph]*, September 2016. arXiv: 1609.08425.

[51] Brian Vlastakis, Gerhard Kirchmair, Zaki Leghtas, Simon E. Nigg, Luigi Frunzio, S. M. Girvin, Mazyar Mirrahimi, M. H. Devoret, and R. J. Schoelkopf. Deterministically Encoding Quantum Information Using 100-Photon Schrödinger Cat States. *Science*, page 1243289, September 2013.

[52] Anthony Chefles. Quantum state discrimination. *Contemporary Physics*, 41(6):401–424, November 2000.

A Appendix

A.1 Analytical results for first replacement stage

In the main text, we have claimed that we find at least one real valued solution for the beam splitter transmissivity to set the overlap in equation (3) to zero. While for our case we find three real valued solutions only one is bounded between zero and one. This is the branch that we consider to implement the physical transmissivities

$$T(\alpha) = \frac{1}{12|\alpha|^4}\left(4|\alpha|^2(3+2|\alpha|^2) - \frac{4(-2)^{1/3}|\alpha|^4(6+|\alpha|^4)}{\left[|\alpha|^6[27-2|\alpha|^2(9+|\alpha|^4)] + 3\sqrt{3}\sqrt{-|\alpha|^{12}\{5+4|\alpha|^2(9+|\alpha|^2+|\alpha|^4)\}}\right]^{1/3}}\right.$$
$$\left. + 2(-2)^{2/3}\left[|\alpha|^6[27-2|\alpha|^2(9+|\alpha|^4)] + 3\sqrt{3}\sqrt{-|\alpha|^{12}\{5+4|\alpha|^2(9+|\alpha|^2+|\alpha|^4)\}}\right]^{1/3}\right) .$$

Furthermore, we give a formula to calculate the success probability for the first replacement stage

$$P_{\text{success}} = e^{-(1-T(\alpha))|\alpha|^2}\left[T(\alpha) + (1-T(\alpha))(1-3T(\alpha))|\alpha|^2 + (1-T(\alpha))^2 T(\alpha)|\alpha|^4\right] .$$

A.2 Generating displaced discrete-variable superposition states

In equation 3, we write the output state of the protocol as the superposition of the vacuum and single photon Fock states, displaced by an amount $\alpha\sqrt{T}$. One solution for equal amplitudes of the two coefficients is achieved when

$$T(\alpha) = \frac{1}{6|\alpha|^2}\left(4\alpha^2 - 2 + \frac{2^{4/3}\alpha^2\left(\alpha^4 - 4\alpha^2 - 2\right)}{b} + 2^{2/3}b\right)$$

where

$$b = \left[3\sqrt{3}\sqrt{3+4\alpha^2+20\alpha^4-4\alpha^6} + \left(7 - 2\alpha^2\left[3 - 6\alpha^2 + \alpha^4\right]\right)\right]^{1/3} .$$